PHYSICAL REVIEW B VOLUME 25, NUMBER 4 15 FEBRUARY 1982

Effect of independent and coupled vibrations of dislocations on low-temperature thermal conductivity in alkali halides

Gary A. Kneezel* and A. V. Granato
Department of Physics, University of Illinois at Urbana-Champaign, Urbana, Illinois 61801
(Received 29 June 1981)

Recent experimental evidence has established that the scattering of phonons by dislocations at low temperatures in [110] LiF rods is primarily a dynamic rather than a static process, but calculations of the effects of vibrating dislocations have failed to provide quantitative agreement with experimental observations of the magnitudes and temperature dependence of the effect. We have performed a calculation which includes many factors previously neglected and show that the effects of resonance angle scattering, phonon focusing, and the resolved shear stress factor have an important influence on the effect of vibrating dislocations on thermal conductivity. However, the detailed calculation shows that in the case of [110] LiF rods the inclusion of these previously neglected factors still does not resolve the discrepancies observed and it is concluded that independently vibrating dislocations are not the important phonon scatterers above 0.1 K in LiF. It is shown, however, that the experimental data may be fit by assuming reasonable densities and distributions of "optically" vibrating dislocation dipoles.

Recent experimental studies by Anderson and co-workers[1,2] have established that the increase in thermal resistivity in LiF at low temperature after plastic deformation is primarily due to dynamic, rather than static, scattering of phonons by dislocations. However, up to now it has not been possible to obtain quantitative agreement between the observed effect and calculations based on either static or dynamic models.[2,3] We present here the results of a detailed calculation based on the dislocation vibrating string model,[4–7] which show that independently vibrating dislocations are not the important phonon scatterers above 0.1 K in LiF, but the experimental data may be fit by assuming reasonable densities of "optically" vibrating dislocation dipoles. As this problem has been a center of interest and controversy for the past 25 years, we will first briefly review the historical background, and further explain the motivation for this investigation.

I. HISTORICAL BACKGROUND

Though they made no reference to the effect of dislocations on thermal conductivity, Eshelby[8] (1949) and Nabarro[9] (1951) made the earliest important contributions by discussing the two mechanisms by which sound waves or phonons are scattered by dislocations. Eshelby proposed that if the sound wave induces the dislocation to vibrate, the incident energy will be dissipated as the dislocation radiates elastic waves. Taking into consideration the wavelength dependence of the effective mass of the dislocation, Nabarro showed that the scattering cross section for this process (reradiation scattering) increases with the wavelength λ, though not as fast as linearly. Even if the dislocation does not vibrate, phonons will be scattered due to the anharmonicity of the dislocation strain field. Nabarro suggested that the scattering cross section for this process (static strain-field scattering) is inversely proportional to λ.

The first detailed treatment of the effects of dislocations on thermal conductivity was given by Klemens[10] in 1955. He considered static strain-field scattering and predicted that the effect would be small even in deformed specimens and would have a temperature dependence of T^2. (If the cross section is proportional to λ^z, the thermal conductivity[11] is proportional to T^{3+z} at low temperatures, and, as Nabarro[9] had suggested, $z=-1$ for this process.)

In 1958, using the reradiation scattering cross section calculated by Nabarro,[9] Granato[12] found that the dynamic scattering by vibrating disloca-

tions should be 3 orders of magnitude greater than Klemens's[10] calculated value of the static scattering at a temperature of 1% of the Debye temperature. Approximating the wavelength dependence of the cross section as $\lambda^{1/2}$, Granato also predicted that the temperature dependence of the thermal conductivity would be $T^{3.5}$.

Shortly thereafter Sproull, Moss, and Weinstock[13] made the first quantitative comparison between thermal resistivity and dislocation density in a nonmetal. For LiF deformed by compression they found the thermal conductivity was approximately proportional to T^2 between 2 and 8 K, as predicted for static strain-field scattering. However the size of the effect was 3 orders of magnitude greater than originally predicted by Klemens's,[10] and 2 orders of magnitude greater than found in Klemens's 1958 calculation.[14]

The measurements of Sproull, Moss, and Weinstock[13] stimulated a large number of theoretical efforts[15–29] to predict a larger magnitude for the static strain-field scattering. However, as pointed out by Granato,[30] a 2 order of magnitude increase in the strain-field-scattering rate would also imply a corresponding 2 order of magnitude increase in the viscous dislocation damping constant, so that the calculated value would be much greater than the measured value.

The reradiation scattering mechanism was ignored for the most part for 10 years after Granato's 1958 paper,[12] although in 1962 Ishioka and Suzuki[31] reaffirmed his conclusion that dynamic scattering is much greater than static scattering. In 1968 Ninomiya,[32] using a more sophisticated formalism, independently calculated the reradiation cross section for the case of phonons incident obliquely onto dislocations. The new feature which this treatment predicts (beyond the normal incidence treatment of Nabarro[9] and Granato[12]) is that at a certain critical angle of incidence the scattering is much greater than at other angles. However, Ninomiya's expressions are very complicated so that the result which has been used[33] in fitting experimental data is that for the case of angles of incidence far from the critical angle—which does not differ significantly from the earlier Nabarro-Granato result.

Actually Nikolayev[7] (1964) treated, prior to Ninomiya, the case of a periodic stress wave incident obliquely onto pinned dislocations in an isotropic solid in an extension of the Granato-Lücke vibrating string model.[5] He did not discuss the resonance angle effect (nor did he explicitly consider reradiation scattering) but an elaboration of his work makes it possible to describe this effect in a simple way as discussed in Sec. II.

The effect of pinning on the reradiation scattering rate was first explicitly considered in 1970 by Garber and Granato.[34] They showed that the scattering due to vibrating pinned dislocations exhibits a resonance peak which rises above the asymptotic value of the scattering predicted for unpinned dislocations, as the resonance is underdamped. At low frequencies the scattering is predicted to decrease to zero in contrast to the divergent behavior predicted for unpinned dislocations. This latter feature was incorporated artificially in 1972 into the Ninomiya formalism[32] by Suzuki and Suzuki,[33] who cut off the scattering at low frequencies. This, however, underestimates the resonance scattering at the peak.

In addition to the theoretical work, further thermal conductivity measurements were made for a variety of deformed alkali halides.[1,2,31,33,35–38] It was found that the temperature dependence at low temperature was T^x with x ranging from less than 2 to greater than 3. This temperature dependence does not clearly favor either static or dynamic scattering.

In 1972 Suzuki and Suzuki[33] presented experimental evidence suggesting that vibrating dislocations were the important source of scattering at low temperatures. After annealing deformed LiF samples at 300 °C for 10 min, they observed that the recovery of the thermal conductivity was greater at lower temperature where the proportion of low-frequency phonons is greater. This is consistent with their interpretation that the dislocations are progressively pinned by point defects during annealing. However, annealing may also cause dislocations to annihilate so that the strain-field scattering would also be expected to decrease.

More direct evidence that pinned vibrating dislocations are the important source of scattering was provided in 1972 by Anderson and Malinowski.[1] They observed that by γ irradiating deformed LiF, the thermal conductivity progressively increased to the undeformed-state value at least for temperature below 1 K. Static scattering by dislocations should be unaffected by irradiation, while dynamic scattering should be affected first at the lowest frequencies (i.e., at the lowest temperatures) and progressively higher with increasing does of irradiation, as was observed by Anderson and Malinowski.

Disturbing discrepancies remained, however.

The average dislocation lengths deduced from thermal conductivity measurements in freshly deformed LiF (Refs. 1 and 2) were much less than those determined ultrasonically.[39] In addition, the observed effect[1,2] was broader than expected, remaining surprisingly large above 2 K. The status of the problem has recently been reviewed by Anderson,[3] who concludes that low-temperature thermal conductivity measurements in deformed LiF are inconsistent with static scattering models but are qualitatively consistent with dynamic scattering models. He observed, though, that it has not been possible to obtain quantitative agreement between experimental data and the calculated effects of reradiation scattering.

However, the qualitative evidence in favor of dominant scattering by vibrating pinned dislocations is so impressive that it raises the question of whether factors previously neglected could account for the discrepancy. It is conceivable that effects such as phonon focusing, the Ninomiya resonance angle effect, and the resolved shear stress factors of the phonons mainly responsible for thermal conductivity could conspire together to produce the observed magnitude and temperature dependence of the effect on the thermal conductivity. Our calculation,[40] outlined in Secs. II and III, includes the following:

(1) the frequency-dependent dislocation effective mass and tension,
(2) the anisotropy of the tension,
(3) the Ninomiya angle resonance effect,
(4) the effect of phonon focusing on each phonon,
(5) the difference in scattering between edge and screw dislocations,
(6) the finite dislocation length,
(7) the rod length-to-width ratio,
(8) the effect of elastic constants of various materials,
(9) the resolved shear stress factor for each incident phonon,
(10) the wavelength dependence of the reradiation scattering,
(11) the calculation for each phonon of boundary scattering plus dislocation scattering,
(12) the dislocation density, and
(13) the rod orientation.

Effects (2), (3), (4), (7), and (9) have not, to our knowledge, been included before in a calculation of the effect of vibrating dislocations on lattice thermal conductivity.

II. THE VIBRATING STRING MODEL FOR WAVES INCIDENT OBLIQUELY ONTO DISLOCATIONS

The calculation on the effect of vibrating dislocations on thermal conductivity divides naturally into two parts. In this section we will consider the frequency dependence of the dislocation scattering rate using parameters appropriate to low-temperature thermal conductivity in alkali halides. In Sec. III we will consider the combined effects of dislocation scattering and boundary scattering[41] on thermal conductivity in the presence of phonon focusing.

A. The unpinned dislocation

Because pinning effects were observed by Anderson and co-workers,[1,2] a realistic treatment must consider the case of pinned dislocations. However, it is useful to consider the case of unpinned dislocations first, as the calculation is easy and the results give simple analytic expressions which are the high-frequency asymptotes for those of the more complicated pinned-dislocation case.

Consider a periodic stress wave $\sigma_p \cos(\vec{k}\cdot\vec{r}-\omega t)$ incident obliquely on an unpinned dislocation lying along the x direction as in Fig. 1. Because the wave is incident obliquely, it hits one end of the dislocation first so that a traveling wave propagates along the dislocation with wavelength $\lambda=\lambda_p/\sin\eta$. If σ_0 is the shear stress component of σ_p resolved in the x-y glide plane in the direction of the Burgers vector $\vec{b}$, the glide force per unit length[42] on the dislocation is $F=b\sigma_0\cos(kx-\omega t)$, where $k=k_p\sin\eta$. The position of the dislocation in the glide plane is $y(x)$. Treating the dislocation as a damped oscillating string with effective mass A, damping constant B, and line tension C, the equation of motion is

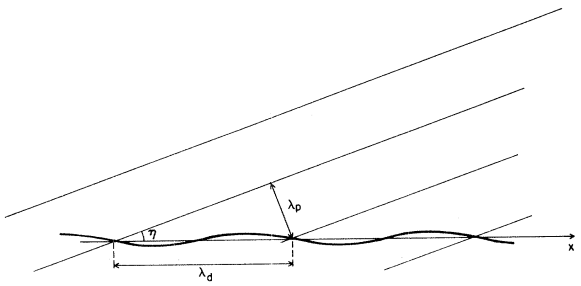

FIG. 1. The excitation of traveling waves along an unpinned dislocation by obliquely incident phonons.

$$A\frac{d^2y}{dt^2}+B\frac{dy}{dt}-C\frac{d^2y}{dx^2}=b\sigma_0\cos(kx-\omega t)\ . \tag{1}$$

Substitution of the trial solution $y=y_i\cos(kx-\omega t)+y_0\sin(kx-\omega t)$ yields

$$y_i=\frac{(-A\omega^2+Ck^2)b\sigma_0}{(-A\omega^2+Ck^2)^2+B^2\omega^2}\ , \qquad y_0=\frac{-B\omega b\sigma_0}{(A\omega^2+Ck^2)^2+B^2\omega^2}\ . \tag{2}$$

The energy lost by the incident wave may be expressed in terms of the logarithmic decrement $\Delta=\Delta W/2W$, where ΔW is the work done on the dislocation per cycle, $W=\sigma_p^2/2G$ is the energy stored per cycle, and G is the appropriate elastic constant. The dislocation strain is $\epsilon_d=\Lambda by$, where Λ is the dislocation density. Then

$$\Delta W=\int\sigma_d de_d=\int\sigma_0\cos(kx-\omega t)\Lambda b\,dy\ ,$$

so that the decrement for unpinned dislocations is

$$\Delta_u=\frac{\pi\Omega\Lambda Gb^2B\omega}{(-A\omega^2+Ck^2)^2+B^2\omega^2}\ , \tag{3}$$

where the resolved shear stress orientation factor is $\Omega=(\sigma_0/\sigma_p)^2$ and takes account of the fact that only the shear stress component on the slip system moves the dislocation.[5,43] The decrement describes how quickly the amplitude of a wave decays. The scattering rate describes the rate at which the incident wave loses its energy to the dislocations and is given by

$$\tau_u^{-1}=\frac{\omega\Delta}{\pi}=\frac{\Omega\Lambda Gb^2s}{\omega A[(R^2-1)^2+s^2]}\ , \tag{4}$$

where $s=B/A\omega$ and $R=(C/A)^{1/2}k/\omega=(C/A)^{1/2}(\sin\eta/v)$. The Ninomiya resonance angle condition[32] corresponds to $R=1$, while the head-on case treated by Granato[12] corresponds to $R=0$. This simple expression for τ_u^{-1} describes the scattering rate for arbitrary angles of incidence and damping.

B. The pinned dislocation

The effect of pinning points at $x=0$ and $x=L$ is to add the boundary conditions $y(0)=y(L)=0$. The Fourier series solution is of the form

$$y=\sum_{m=1}^{\infty}A_m\sin k_mx\cos\omega t+B_m\sin k_mx\sin\omega t\ , \tag{5}$$

where $k_m=m\pi/L$. The decrement is

$$\Delta(x)=\frac{1}{2W}\int\sigma_d(x)d\epsilon_d(x)\ , \tag{6}$$

$$\Delta=\frac{1}{L}\int_0^L\Delta(x)dx\ . \tag{7}$$

The result is $\Delta=\sum_{m=1}^{\infty}\Delta_m$, where

$$\Delta_m=\frac{4\Omega\Lambda Gb^2L^2}{\pi^3C}\left[\frac{1}{m(m^2-R^2u^2)}\right]^2\times\frac{su^2[1-(-1)^m\cos\pi Ru]}{[(1-u^2/m^2)^2+(su^2/m^2)^2]}\ . \tag{8}$$

In Eq. (8), u is the normalized frequency ω/ω_1, and ω_m is the mth normal mode resonant frequency given by $\omega_m=m\pi/l(C/A)^{1/2}$. Nikolayev gives a similar result.

C. Parameters of the model

1. *Effective mass A*

The effective mass[44] is $A=(\rho'b^2/4\pi)\ln g$, where $\rho'=\rho$ (the density of the solid) for a screw dislocation and $\rho'=\rho[1+(c_t/c_l)^4]$ for an edge dislocation where c_t and c_l are the transverse and longitudinal velocities of sound. At low frequencies g is given by R_0/r_0, where R_0 and r_0 are the upper and lower cutoff distances for the dislocation strain fields so that $g\sim1/\sqrt{\Lambda}b$. For high frequencies the wavelength or frequency dependence of the mass becomes important and Eshelby[44] gives $g=1+\omega_{\max}/\omega$, where $\omega_{\max}$ may be approximated by the Debye frequency ω_D.

2. *Line tension C*

The line tension is given in terms of the energy per length of dislocation line by $C=E+d^2E/d\psi^2$, where ψ is the angle between $\vec{b}$ and $\vec{x}$. An anisotropic calculation of C for NaCl structure materials may be performed in the same way as by deWit and Koehler[45] and by Stern and Granato[46] for fcc materials. In an anisotropic cubic solid, Foreman[47] has shown that (neglecting the dislocation core) $E=Kb^2/4\pi\ln(R_0/r_0)$. For dislocations on the (110) planes (the NaCl structure slip planes) it may be shown that for screw dislocations $K_s=(C_{44}C')^{1/2}$, while for edge dislocations $K_e=\alpha K_s$, where

$$\alpha=\left[\frac{2(C_{11}+C_{12})^2}{C_{11}(C_{11}+C_{12}+2C_{44})}\right]^{1/2}. \tag{9}$$

Huntington, Dickey, and Thomson[48] evaluated K numerically for intermediate angles in NaCl and found the results could be fit by $E=E_0+E_1\cos 2\psi$. Thus $C=(\gamma b^2/4\pi)\ln(R_0/r_0)$, where the maximum value of γ is $\gamma_s=K_s(2\alpha-1)$, while the minimum value is $\gamma_e=K_s(2-\alpha)$. At high frequency, the tension, like the mass, depends on the frequency and again we assume $g=1/\sqrt{\Lambda}b$ or $1+\omega_D/\omega$, whichever is less.

3. Damping constant B

At low temperatures in insulators at thermal phonon frequencies, the damping constant is due almost entirely to the reradiation damping mechanism.[30] Eshelby[44] calculated the rate of radiation from a dislocation vibrating as a rigid rod in an isotropic solid to yield the results $B_s=(\rho b^2\omega/8)$ and $B_e=B_s[1+(c_t/c_l)^4]$ for screw and edge dislocations, respectively. Because we are considering the general case of oblique incidence, giving rise to spatially sinusoidal dislocation vibration, it is more appropriate to use the results of the calculation of Laub and Eshelby[49] for the rate of radiation from a sinusoidal dislocation. Recalling that the wave vector is $k=(\omega\sin\eta/v$, we may express their $k\neq 0$ results in terms of the quotient $Q(k)=B(k)/B(0)$ for screw and edge dislocations:

$$Q_s(k)=\begin{cases}1-\dfrac{3c_t^2\sin^2\eta}{v^2}+\dfrac{4c_t^4\sin^2\eta}{v^2c_l^2}\,, & \sin\eta\le v/c_l\\[2ex] 1-\dfrac{3c_t^2\sin^2\eta}{v^2}+\dfrac{4c_t^4\sin^4\eta}{v^4}\,, & v/c_l\le\sin\eta\le v/c_t\\[2ex] 0\,, & v/c_t<\sin\eta\end{cases} \tag{10}$$

$$Q_e(k)=\begin{cases}1-\dfrac{2\sin^2\eta}{v^2c_l^2(1/c_t^4+1/c_l^4)}\,, & \sin\eta\le v/c_l\\[2ex] 1-\dfrac{(1/c_l^4+\sin^4\eta/v^4)}{(1/c_l^4+1/c_t^4}\,, & v/c_l\le\sin\eta\le v/c_t\\[2ex] 0\,, & v/c_t<\sin\eta\,.\end{cases} \tag{11}$$

Cubic solids do not have a single shear velocity c_t and a single longitudinal velocity c_l. We choose c_t to be the minimum shear velocity (the slow transverse velocity along [110]) and c_l to be the longitudinal velocity along [001].

4. Resonance angle ratio R

Using the above expressions for C and A we find for screw and edge dislocations:

$$R_s=\left[\frac{K_s(2\alpha-1)}{\rho}\right]^{1/2}\frac{\sin\eta}{v}\,, \tag{12}$$

$$R_e=\left[\frac{K_s(2-\alpha)}{\rho[1+(c_t/c_l)^4]}\right]^{1/2}\frac{\sin\eta}{v}\,. \tag{13}$$

The resonance angle condition is fulfilled at $R=1$. In agreement with Ninomiya[32] it is found that the condition $R_e=1$ (for edge dislocations) cannot be fulfilled for $\sin\eta\le 1$. In addition, $R=1$ cannot be fulfilled for screw dislocations if v is too large (e.g., if the phonon is longitudinal).

5. Resolved shear stress orientation factor Ω

For arbitrary mode waves incident on dislocations in arbitrary slip systems, expressions such as (3), (4), and (8) may retain their simple form if the expression for Ω is modified. Following the procedure used by Green and Hinton[50] for fcc metals, we find for slip systems S in alkali halides:

$$\Omega_S=\frac{-\Lambda_S C' F_S^2 k^2 a^2}{2W\Lambda}\,, \tag{14}$$

where a is the wave amplitude, Λ_S is the dislocation density on slip system S, and $\Lambda=\sum\Lambda_S$. The slip systems and F_S^2 are given in Table I, as well as Ω for the pure mode [110] phonons. The stored elastic energy per cycle is

$$W=\tfrac{1}{2}\sigma_{ij}\epsilon_{ij}=-\tfrac{1}{2}k^2a^2\{C_{11}(\alpha^2l^2+\beta^2m^2+\gamma^2n^2)+2C_{12}(\alpha\beta lm+\alpha\gamma ln+\beta\gamma mn) +C_{44}[(\alpha m+\beta l)^2+(\alpha n+\gamma l)^2+(\beta n+\gamma m)^2]\}\ , \tag{15}$$

where the wave vector is $\vec{k}=k[lmn]$ and the polarization vector is $[\alpha\beta\gamma]$.

6. *Distribution of dislocations loop length L*

Because the pinning points on the dislocations are expected to be randomly distributed, the decrement (or scattering rate) must be averaged over loop lengths.[4] The integration in (16) must be done numerically:

$$\Delta=\frac{1}{L^2}\int_0^\infty l\exp(-l/L)\Delta(l)\,dl\ , \tag{16}$$

where L is the average dislocation loop length.

7. *Dislocation density* Λ

The most direct measurements of dislocation density are by electron microscopy and by etch-pit studies. Johnston and Gilman's classic etch-pit studies[51] in LiF suggested that $\Lambda\sim10^9\epsilon_p$ for plastic strain ϵ_p in the range $10^{-3}-10^{-1}$. Both electron microscopy and etch-pit studies lead to estimates of the ratio of edge-to-screw dislocations. However, many of the etch pits on edge-type surfaces may be due to debris (dislocation dipoles and deformation-induced point defects) rather than isolated dislocations.[52] Most edge dislocations appear to be present as close pairs of opposite sign (dislocation dipoles and higher-order multipoles), while most screw dislocations are unpaired.[53]

D. Decrement and scattering-rate curves

Figure 2 shows the normalized decrement $\Delta/\Omega\Lambda L^2=\sum\Delta_m$ (summed over the first 80 modes) as well as the individual contribution of the first mode and the 25th mode assuming $R=0$, $Q=1$, all the dislocations are the same length L, and the frequency is low enough that the mass and line tension are not frequency dependent. The unpinned dislocation asymptote is also shown and is approached to within 10% by $\omega/\omega_1=30$. Figure 3 is similar except for $R=1$ (the Ninomiya resonance angle). In the head-on incident case (Fig. 2) it can be seen that the contribution of the first term alone Δ_1 is a good approximation to the decrement for the pinned dislocation as originally observed by Granato and Lücke.[5] At the fundamental resonant frequency ω_1, the decrement is nearly 2 orders of magnitude greater than that calculated for the un-

TABLE I. Slip systems and F_S^2 for NaCl structure alkali halides and orientation factors for [110] propagation vector phonons.

S	Slip system	F_S^2	Ω_l	$\Omega(C_{44})$	$\Omega(C')$
1	$(110)[1\bar{1}0]$	$(\alpha l-\beta m)^2$	0	0	$\frac{\Lambda_S}{\Lambda}$
2	$(1\bar{1}0)[110]$	$(\alpha l-\beta m)^2$	0	0	$\frac{\Lambda_S}{\Lambda}$
3	$(101)[10\bar{1}]$	$(\alpha l-\gamma n)^2$	$\frac{\Lambda_S C'}{2\Lambda(C_{11}+C_{12}+2C_{44})}$	0	$\frac{\Lambda_S}{4\Lambda}$
4	$(10\bar{1})[101]$	$(\alpha l-\gamma n)^2$	$\frac{\Lambda_S C'}{2\Lambda(C_{11}+C_{12}+2C_{44})}$	0	$\frac{\Lambda_S}{4\Lambda}$
5	$(011)[01\bar{1}]$	$(\beta m-\gamma n)^2$	$\frac{\Lambda_S C'}{2\Lambda(C_{11}+C_{12}+2C_{44})}$	0	$\frac{\Lambda_S}{4\Lambda}$
6	$(01\bar{1})[011]$	$(\beta m-\gamma n)^2$	$\frac{\Lambda_S C'}{2\Lambda(C_{11}+C_{12}+2C_{44})}$	0	$\frac{\Lambda_S}{4\Lambda}$

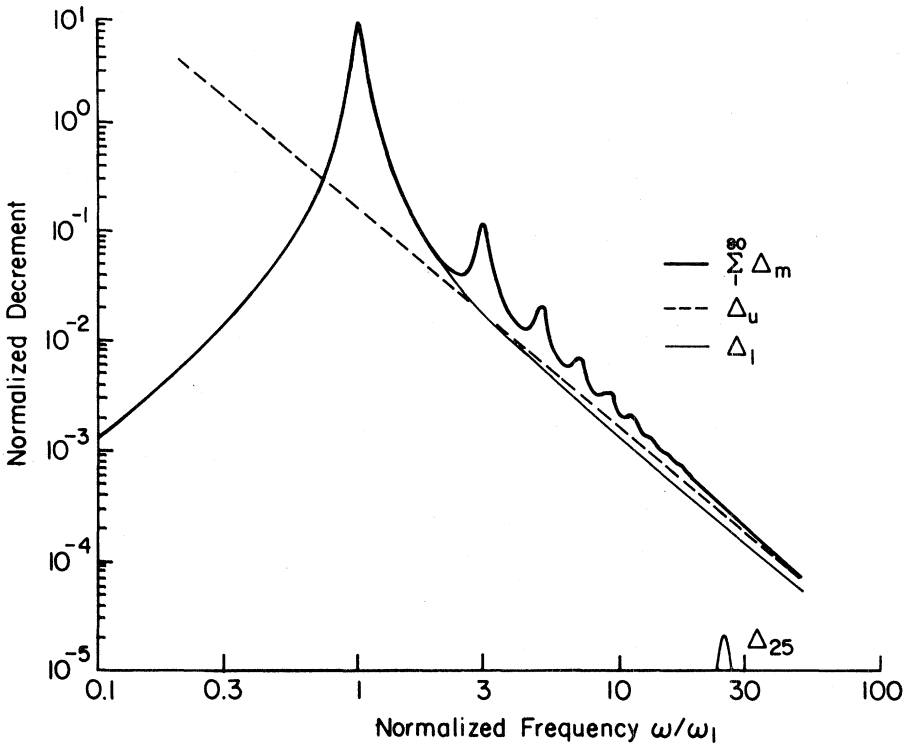

FIG. 2. The normalized decrement $\Delta/\Omega\Lambda L^2$ vs the normalized frequency ω/ω_1 for head-on incidence ($R=0$). Shown are the decrement summed over the first 80 normal modes $\sum^{80}\Delta_m$, as well as the individual contributions of the first mode (Δ_1) and the 25th mode (Δ_{25}), and the decrement for an unpinned dislocation Δ_u.

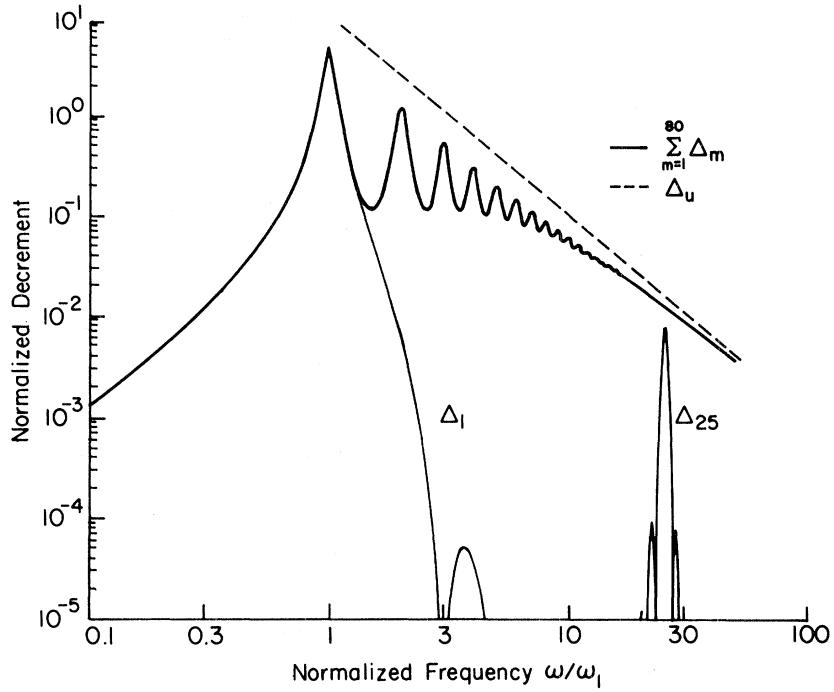

FIG. 3. The normalized decrement $\Delta/\Omega\Lambda L^2$ vs the normalized frequency ω/ω_1 for the Ninomiya resonance angle ($R=1$). Shown are $\sum^{80}\Delta_m$, Δ_1, Δ_{25}, and Δ_u.

pinned dislocation because the unpinned dislocation is not at resonance. If the unpinned dislocation is at resonance (the Ninomiya angle resonance) as in Fig. 3, the effect of pinning is to inhibit the dislocation from vibrating as freely so that the decrement of the pinned dislocation is less than that of the unpinned dislocation. For the $R=1$ case it can also be seen that the first mode contribution is a good approximation only up to $1.5\omega_1$ and the major contribution at a given frequency is due to the mode which is resonant near that frequency. At frequencies greater than $2\omega_1$, the decrement is much greater for the $R=1$ case than for the $R=0$ case, while at ω_1 the $R=0$ decrement is slightly greater, and at low frequencies they are the same. There is negligible difference at $\omega << \omega_1$ because the stress wavelength is large so that the variation in stress along the dislocation is small regardless of the angle of incidence. The first mode contribution is dominant at such low frequencies because the nearly constant stress primarily excites the longest wavelength mode.

Figure 4 shows the normalized scattering rate $\tau^{-1}/2\omega_1\Omega\Lambda L^2$ for the same assumptions as above (for $R=0$, 0.8, 1.0, and 1.2) but averaged over the Koehler distribution[4] of loop lengths. It may be seen that the averaging smears out the peak structure, but an enhancement near the maximum with respect to the unpinned dislocation asymptote remains for the $R\neq 1$ curves. The pronounced peak is due to the undamped character of the resonance. Although the resonance angle enhancement is greatest at $R=1$, it is still considerable at $R=0.8$ and $R=1.2$.

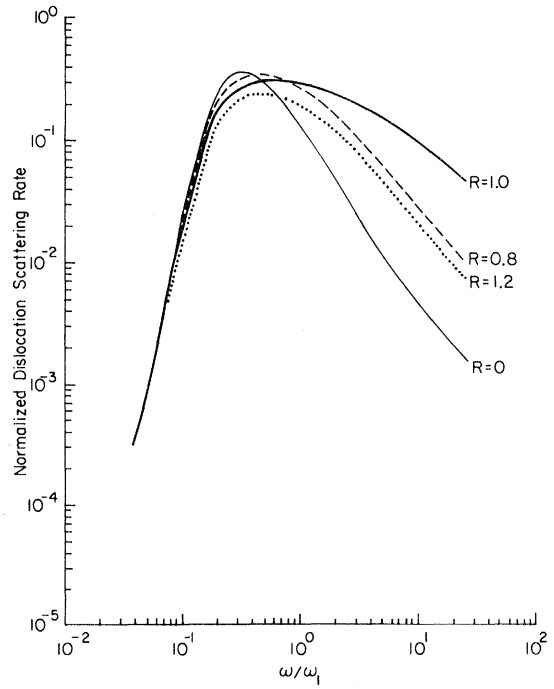

FIG. 4. The normalized scattering rate $\tau^{-1}/2\omega_1\Omega\Lambda L^2$ vs the normalized frequency ω/ω_1, averaged over the Koehler distribution of dislocation lengths for $R=0$, 0.8, 1.0, and 1.2. The frequency dependence of the dislocation mass and tension is neglected.

The curves of Fig. 4 do not include the frequency dependence of the dislocation mass and tension. Figure 5 shows the normalized scattering rate including this effect for the case $\omega_D=1000\omega_1$. It may be seen in comparison with Fig. 4 that the high-frequency side of the peak is enhanced for the $R\neq 1$ curves. The frequency dependence of the mass and line tension has no effect on the $R=1$ curve at high frequency, as can be seen by rewriting Eq. (4) as

$$\tau_u^{-1}=\frac{8\Omega\Lambda GQ}{\rho\omega\{[(2/\pi)(R^2-1)\ln g]^2+Q^2\}} . \tag{17}$$

For the unpinned dislocation at resonance ($R=1$) the scattering rate is determined by the damping alone so that the frequency dependence of the mass and tension is not important in this limit. For $R\neq 1$, however, the enhancement is large at high frequencies.

For both Figs. 4 and 5 it is assumed that $Q=1$, that is, the wavelength dependence of the reradiation damping constant is neglected. Figure 6 shows for the intermediate $R=0.8$ case, the normalized scattering rate for $Q=0.5$, 1, 1.5, 2. The wavelength dependence of B is seen to have a smaller influence than the resonance angle effect and the frequency dependence of C and A.

To obtain the scattering rate from the normalized scattering-rate curves one must multiply by $2\Omega\Lambda\omega_1 L^2$. The effects of Λ and Ω are straightforward: a larger scattering rate comes from a larger density of dislocations and/or a larger orientation factor. The effect of average length is shown in Fig. 7. The frequency at which maximum scattering occurs is inversely proportional to L, while the magnitude of the maximum is proportional to L.

III. EFFECT OF INDEPENDENTLY VIBRATING DISLOCATIONS ON THERMAL CONDUCTIVITY

In insulators and superconductors the conduction of heat is via phonons.[11] At the lowest tem-

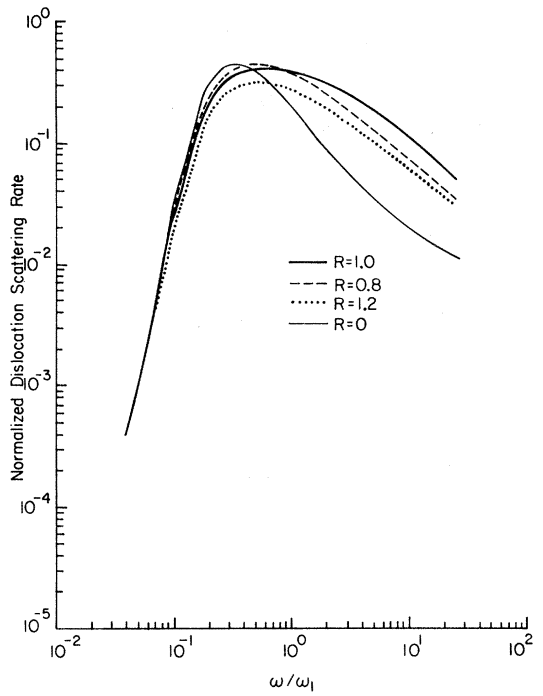

FIG. 5. The normalized scattering rate $\tau^{-1}/2\omega_1\Omega\Lambda L^2$ vs the normalized frequency ω/ω_1, averaged over the Koehler distribution of dislocation lengths for $R=0$, 0.8, 1.0, and 1.2. The frequency dependence of the dislocation mass and tension is included for the specific case $\omega_D=1000\omega_1$.

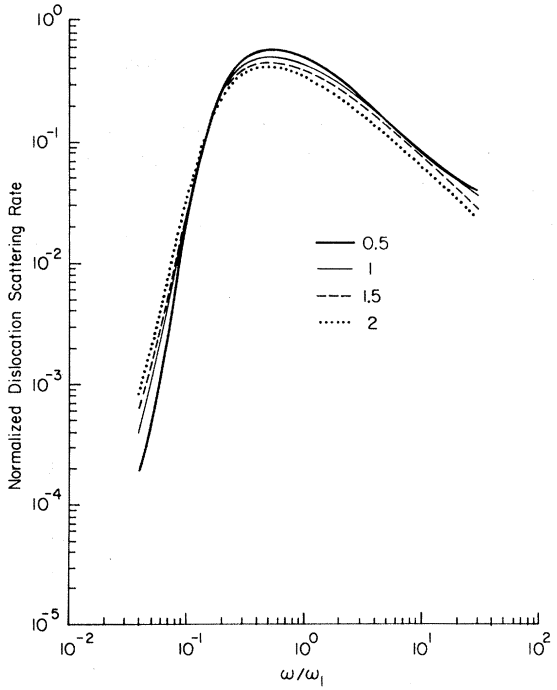

FIG. 6. The normalized scattering rate vs the normalized frequency for $R=0.8$; $\omega_D=1000\omega_1$; and $Q=0.5$, 1, 1.5, and 2.

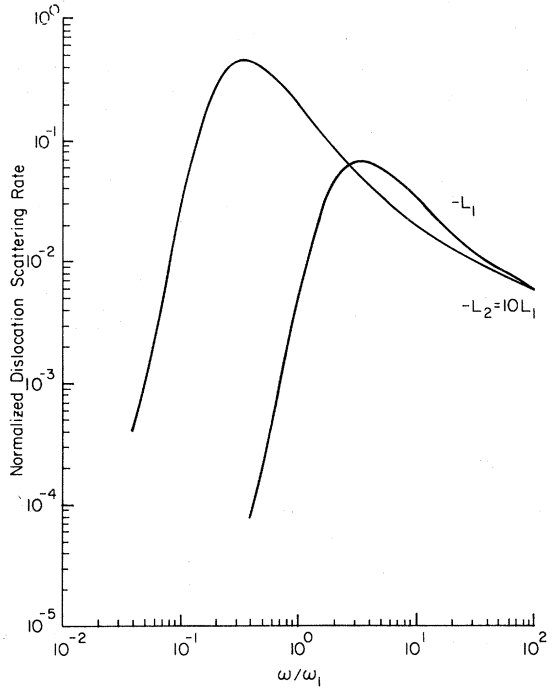

FIG. 7. The normalized scattering rate $\tau^{-1}/2\omega_1(L_2)\Omega\Lambda L_2^2$ vs the normalized frequency $\omega/\omega_1(L_2)$ for average dislocation lengths L_1 and $L_2=10L_1$. Here it is assumed $R=0$, $Q=1$, and $\omega_D=1000\omega_1(L_2)$.

perature the limit to thermal conductivity is due to scattering of phonons by the surface of the sample[41] (boundary scattering) and by lattice defects.[11] In this section we will consider boundary scattering and reradiation scattering in an anisotropic solid, explicitly including phonon focusing, and compare the results to experimental results in LiF.

A. Boundary scattering-limited thermal conductivity

There are several approaches[54–57] to the problem of the effect of phonon focusing on boundary scattering-limited thermal conductivity, but the one which may be extended most easily to include reradiation scattering is that of McCurdy, Maris, and Elbaum.[54] In a relaxation-time approximation, the thermal conductivity per volume is[16]

$$K=\left[\frac{1}{2\pi}\right]^3\sum_j\int q^2\tau_j(q)C_{\rm ph}V_j^2(q)\times\cos^2\theta_g\sin\theta\,dq\,d\theta\,d\phi\ , \quad (18)$$

where $\vec{q}$ is the phonon wave vector having coordinates (q,θ,ϕ) with respect to the rod axis, j is the polarization index, V is the group velocity making an angle θ_g with the rod axis, τ is the reciprocal of the scattering rate, and

$$C_{\rm ph}=\frac{(\hbar\omega)^2\exp(\hbar\omega/kT)}{kT^2[(\exp(\hbar\omega/kT)-1]^2}\ . \tag{19}$$

The collision free path in a square-cross-section rod of side D is given by[58]

$$\Lambda_j(q)=\tau_j(q)V_j(q)=\begin{cases}\dfrac{D}{6}\dfrac{3|\cos\phi_g|-|\sin\phi_g|}{\sin\theta_g\cos^2\phi_g}\ , & |\cos\phi_g|>|\sin\phi_g| \\ \dfrac{D}{6}\dfrac{3|\sin\phi_g|-|\cos\phi_g|}{\sin\theta_g\sin^2\phi_g}\ , & |\sin\phi_g|>|\cos\phi_g| \\ \dfrac{D}{6}F(\theta_g,\phi_g)\ .\end{cases} \tag{20}$$

The thermal conductivity may be written as $K=\frac{1}{3}C\bar{v}\bar{l}$, where C is the specific heat, $\bar{v}$ is the average phase velocity, and $\bar{l}$ is the mean free path. Defining the quantities $\langle v^{-n}\rangle$ and $\langle V/v^3\rangle$ as

$$\langle v^{-n}\rangle=\frac{1}{3}\sum_j\frac{1}{4\pi}\int\frac{\sin\theta\,d\theta\,d\phi}{v_j^n(\theta,\phi)}\ , \tag{21}$$

$$\left\langle\frac{V}{v^3}\right\rangle=\frac{1}{3}\sum_j\frac{1}{4\pi}\int\frac{V_j\cos^2\theta_g F(\theta_g,\phi_g)\sin\theta\,d\theta\,d\phi}{v_j^3(\theta,\phi)}\ , \tag{22}$$

the average velocity and mean free path may be expressed as

$$\bar{v}=\frac{\langle v^{-2}\rangle}{\langle v^{-3}\rangle}\ ,\quad \bar{l}=\frac{D}{2}\frac{\langle V/v^3\rangle}{\langle v^{-2}\rangle}\ . \tag{23}$$

We may get an indication of the contribution of each mode j to the mean free path by defining

$$\bar{l}_j=\frac{D}{6}\frac{\langle V/v^3\rangle_j}{\langle v^{-2}\rangle_j}\ . \tag{24}$$

The total mean free path is

$$\bar{l}=\frac{D}{2}\sum_j\left\langle\frac{V}{v^3}\right\rangle_j\Big/\sum_j\langle v^{-2}\rangle_j\neq\sum_j\bar{l}_j\ , \tag{25}$$

but $\bar{l}\sim\sum\bar{l}_j$ turns out to be a reasonable approximation. In particular, a numerical calculation with $\Delta\theta=\Delta\phi=\frac{1}{2}^\circ$ for a [110] LiF rod gives $\bar{l}=1.33D$, while $\sum_j\bar{l}_j=\bar{l}_L+\bar{l}_{\rm FT}+\bar{l}_{\rm ST}=(0.41+0.65+0.29)D=1.35D$. Notice that due to phonon focusing the fast transverse mode (FT) makes the largest contribution to the mean free path in this case. Figure 8 shows schematically the focusing of phonons along [110] in LiF.

We have overestimated the mean free path (especially of the fast transverse mode) by implicitly assuming the rod is of infinite length. A simple finite-rod correction is to assume Λ_j is given by the rod length or by Eq. (20), whichever is less. The result of this correction for length-to-width ratio of 7.5 is $\bar{l}=0.99D$, while $\sum_j\bar{l}_j=(0.35+0.38+0.28)D=1.01D$.

B. Boundary scattering plus reradiation scattering

In order to include the effects of dislocation scattering we simply add the boundary scattering and reradiation scattering rates for each phonon, i.e., $\tau^{-1}=\tau_B^{-1}+\tau_d^{-1}$. The boundary scattering rate is

$$\tau_{B_j}^{-1}(q)=6V_j(q)/DF(\theta_g,\phi_g)\ . \tag{26}$$

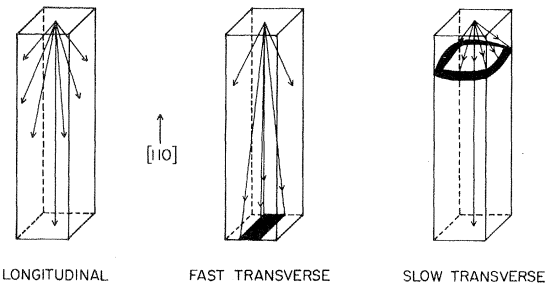

FIG. 8. Schematic representation of phonon focusing of the three modes in a [110] LiF rod.

The calculation proceeds as follows: a set of master scattering-rate curves for various Q, R, and ω_D/ω_1 is calculated. For the chosen material the dislocation effective mass and tension are calculated from material constants. For a particular average dislocation length ω_1 is calculated. Given the Debye frequency we can interpolate between the various ω/ω_1 curves. A density of a particular type of dislocation is assumed and the angle of incidence, Q, R, and Ω, is calculated for each phonon. Interpolation is done between the master Q and R scattering-rate curves to give the dislocation scattering rate τ_d^{-1}. This is done for each of the three phonon modes with angle intervals $\Delta\theta=\Delta\phi=1°$.

Because τ_d^{-1} changes relatively slowly with frequency we may make the dominant-phonon approximation[1] which assumes that at temperature T the dominant-phonon frequency is the peak of $\omega^2 C_{\rm ph}$ and is given by

$$\omega_{\rm dom}=\frac{3.8kT}{\hbar}=5.0\times10^{11}T\ . \tag{27}$$

Thus if we plot the calculated mean free path versus frequency, the relation $T=2\times10^{-12}\omega$ may be used to indicate the corresponding temperature.

C. Influence of the frequency-dependent mass, the Ninomiya resonance, and the wavelength dependence of reradiation damping

Figure 9 illustrates the influence of including the assumptions of a frequency-dependent dislocation mass, the Ninomiya resonance angle effect, and the wavelength dependence of the reradiation damping [denoted, respectively, by $A(\omega)$, R, and Q]. The ratio of mean free path l in the deformed sample to mean free path l_B for boundary scattering alone is plotted versus frequency. The parameters assumed to be held constant in these curves are as follows: (a) the sample is a 3-cm long by 0.2-cm wide LiF square-cross-section rod oriented along [110]; (b) there are 2.5×10^7-cm^{-2} screw dislocations of average length 3×10^{-6} cm situated on any or all of the (101), (10$\bar{1}$), (011), or (01$\bar{1}$) planes (hereafter designated collectively as {101}); (c) phonon focusing and the resolved shear stress orientation factor are calculated for each of the 24 300 phonons ($3\times90\times90$) considered in the octant. As can be seen, the effect of the $A(\omega)$ and R assumptions is to broaden the frequency dependence of the mean free path and shift the minimum to higher frequency. The most important influence is the

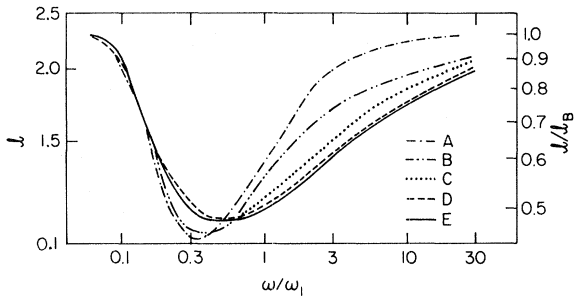

FIG. 9. The calculated mean free path vs frequency for boundary scattering plus dislocation scattering in a 3-cm long by 0.2-cm-wide square-cross section [110] LiF rod, assuming 2.5×10^7-cm^{-2} screw dislocations on the {101} planes and including phonon focusing and the resolved shear stress factor for each phonon. (A) The resonance angle effect R, the frequency dependence $A(\omega)$ of the dislocation mass and line tension, and the wavelength dependence Q of the reradiation damping constant are all neglected. (B) $A(\omega)$ is included; R and Q are not. (C) R is included; $A(\omega)$ and Q are not. (D) $A(\omega)$ and R are included; Q is not. (E) $A(\omega)$, R, and Q are all included.

Ninomiya angle resonance which has been assumed negligible in previous calculations. The effect of Q is comparatively small, but all three assumptions are included hereafter to make the curves as realistic as possible.

D. Combined effects of phonon focusing and the resolved shear stress orientation factor

Phonon focusing and the resolved shear stress factor are anisotropic and mode dependent and must be considered together as illustrated in Fig. 10. Figure 10(a) is plotted for the same assumptions as Fig. 9(E) but is separated according to the contribution of each mode, the horizontal lines representing the contribution for boundary scattering alone. Because the fast transverse mode is focused more strongly along [110] than longitudinal or slow transverse, its contribution to the mean-free path is dominant. In LiF, where the fast transverse mode is C_{44}, dislocation scattering has a relatively weak effect because the C_{44} mode is weakly scattered. The fast transverse mode scattering is not zero (as would be suggested by Table I for the [110] pure mode), emphasizing that the resolved shear stress factor must be calculated for each phonon.

The difference in scattering for C'- and C_{44}-like phonons is demonstrated more clearly for disloca-

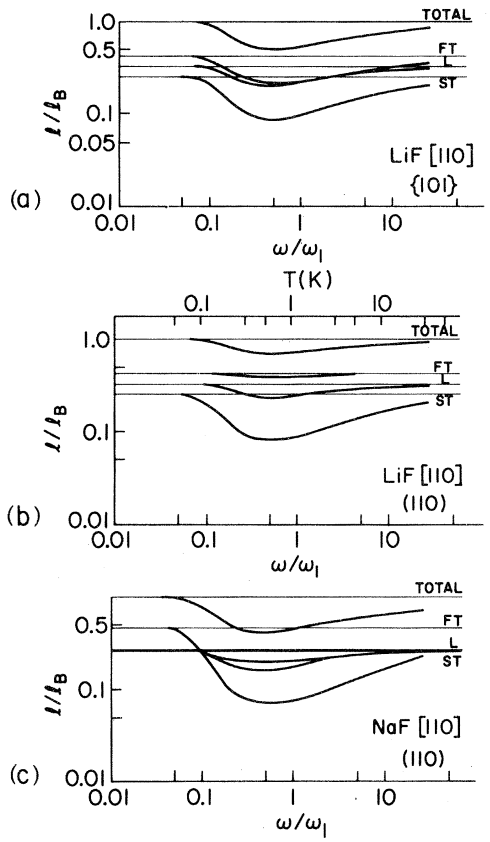

FIG. 10. The mean free path vs frequency and temperature for boundary scattering and boundary scattering plus dislocation scattering for each model. (a) LiF [110]: screw dislocations on {101} slip planes. (b) LiF [110]: screw dislocations on (110) slip planes. (c) NaF [110]: screw dislocations on (110) slip planes.

tions on the (110) planes as seen in Fig. 10(b), where the assumptions are the same as in Fig. 10(a) except for slip planes. Here the dominant fast transverse phonons are very weakly scattered while the slow transverse phonons are very strongly scattered. This has two important results. First, the size of the effect is smaller and the curve is flatter for dislocation on (110) as compared to {101}. Second, there is a saturation effect as suggested by Anderson and Malinowski.[1] Due to a certain density of dislocations, the contribution of the strongly scattered slow transverse phonons becomes negligible. Adding more dislocations does not decrease the minimum mean free path appreciably, the remaining phonons being more weakly scattered. Thus the minimum mean free path changes more slowly with dislocation density for dislocations on (110) as compared to {101}.

In NaF the fast transverse mode is the C' mode and again in the absence of dislocation scattering the fast transverse mode is dominant due to phonon focusing. As shown in Fig. 10(c), this implies that the dislocation scattering effects should be much greater for a given density of dislocations on (110) in NaF as compared to LiF.

E. Attempt to fit experimental data

Figure 11 shows the ratio of the thermal conductivity of a bent [110] LiF rod to that before deformation as measured by Roth and Anderson.[2] The dislocation density was determined to be about 2.5×10^7 cm^{-2} by etch-pit counts. Also shown in Fig. 11 are the calculated l/l_B curves calculated for 2.5×10^7-cm^{-2} screw dislocations on the (110) planes and on the {101} planes. An average dislocation length of 6×10^{-6} cm was assumed in order to produce a scattering-rate peak at a frequency corresponding to the observed thermal conductivity minimum near 0.25 K. This length is a factor of 3 less than that determined ultrasonically by Wire.[39] (Owing to the lower line tension and larger mass for edge dislocations an average length of 4×10^{-6} cm would be required assuming all edge dislocations.) In addition it can be seen that the calculated effect is not as large as was observed—especially in view of the fact that bending the [110] rod about the [001] axis should have produced dislocations mainly on the (110) planes.

In conclusion, the results of the detailed calculation show that in [110] LiF the various factors do not conspire together to produce an effect as large as observed (although in [110] NaF they would to a greater extent). In addition, for a dislocation

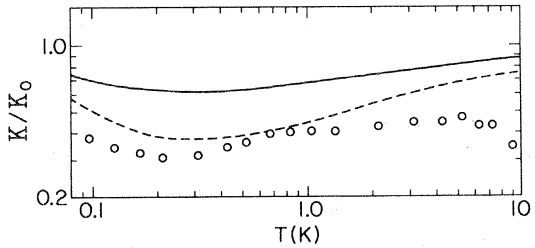

FIG. 11. ○: Measured (Ref. 2) ratio of thermal conductivity κ/κ_0 in a bent LiF [110] rod to that before deformation. —: Calculated ratio of dislocation plus boundary scattering mean free path to boundary scattering mean free path for dislocations on (110). — — —: Calculated l/l_B for dislocations on {101}.

length 2×10^{-5} cm, as observed ultrasonically,[39] the minimum in thermal conductivity would occur near 0.07 K.

The results suggest the data could be fit better by assuming a dislocationlike defect having a higher resonant frequency and being more numerous than isolated dislocations. As shown in Sec. IV these conditions are met by the optically vibrating edge dislocation dipole.

IV. EFFECT OF VIBRATING EDGE DISLOCATION DIPOLES ON THERMAL CONDUCTIVITY

Two dislocations of opposite sign on parallel glide planes a distance d apart have a stable configuration when they are a distance of $\sqrt{2}d$ apart[58] and the pair is called a dislocation dipole. Because screw dislocations are able to cross glide and annihilate, the great majority of dipoles are of edge character.

A. Density of distribution of edge dipoles

Dislocation dipoles were first observed and discussed by Johnston and Gilman[52] in their etch-pit studies in LiF. They suggested that the approximate range of dipole spacings is $3b \leq d \leq 300$b. Estimates of the density of dipoles and distribution of spacings are difficult. If the etch pits get close together they cannot be resolved. More importantly, because etching occurs primarily at the strained region of the crystal, narrow dipoles may not etch at all,[36] the strained region being confined to the space between the pair. Similarly it is difficult to see very narrow dipoles via electron microscopy.[59] Estimates of the ratio of the dislocation dipole density to monopole density range from 1000 (Gilman[60]—strain-hardening measurements) to 100 (Davidge and Pratt[61]— deformation-induced bulk-density changes) and less (electron microscopy).[62,63] A reasonable ratio appears to be 10—100, distributed primarily at spacings of 3—300 b, with most having spacings less than a few hundred Angstroms so that they are not easily detected by electron microscopy or etch-pitting techniques. A distribution of this character (for $d=nb$) is the exponential distribution $\Lambda(n)=\Lambda_0\exp[-(n-3)/N_0]$ for $n\geq3$.

B. Optical mode resonant frequency

Long-wavelength phonons ($\lambda>>d$) will excite dipoles into the optical mode of vibration (i.e., the dislocations move in opposite directions). For small oscillations a linear term Dy is added to the left side of the equation of motion (1). The resonance frequency of the mth normal optical mode is

$$\omega_{\rm op}(m)=\left[\omega_{\rm ac}^2(m)+\frac{D}{A}\right]^{1/2}=\left[\frac{m^2\pi^2}{L^2}\frac{C}{A}+\frac{D}{A}\right]^{1/2}, \tag{28}$$

here $\omega_{\rm ac}$ is the acoustical mode resonant frequency, A is the effective mass, C is the tension, and

$$D=\frac{Gb^2}{2\pi(1-\nu)d^2}\ . \tag{29}$$

Thus the optical mode resonant frequency is higher than the acoustical mode resonant frequency, especially for narrow dipoles.

C. Fit to experimental data

Dipole scattering rates were averaged over dipole spacings and lengths with two simplifying assumptions: (a) the dislocations exhibit coupled oscillations (dipole optical mode) for long-wavelength phonons (specifically $\omega<2\omega_1$) but oscillate independently at shorter wavelengths; and (b) pinning points are similarly situated on both dislocations of a dipole.

It was found that by assuming an average dipole spacing $N_0b=60$ b the minimum could be properly situated at 0.25 K for an average dislocation length of 2×10^{-5} cm, as determined ultrasonically.[39] Figure 12 shows Roth and Anderson's[2] thermal conductivity data in the deformed sample of Fig. 11 subsequently irradiated. Also shown are curves calculated with Eq. (28), assuming dislocation

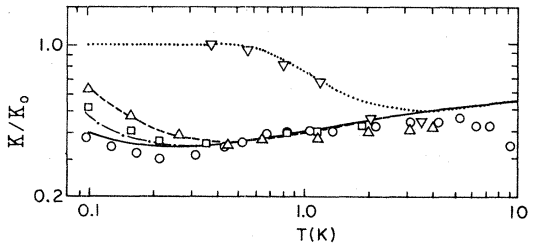

FIG. 12. Measured (Ref. 2) κ/κ_0 before and after irradiation, and calculated l/l_B for edge dislocation dipoles with $N_0=60$ and various average lengths. ○: Freshly bent sample; —: $L=2\times10^{-5}$ cm; □: After 720-R γ irradiation; —·—·—·: $L=1\times10^{-5}$ cm; △: 2100 R; — — —: $L=5\times10^{-6}$ cm; ▽: 180 000 R; · · · : $L=8\times10^{-8}$ cm.

lengths of 2×10^{-5} cm, 1×10^{-5} cm, 5×10^{-6} cm, and 3×10^{-7} cm and a density of 7.5×10^{8}-cm^{-2} edge dipoles on the (110) planes. These values of L should be expected[65] to correlate with

$$L=L_0/(1+\beta t)\ , \tag{30}$$

where L_0 is the length before radiation, t is the radiation time, and β is a constant. The first three lengths (2, 1, and 0.5×10^{-5} cm) are consistent with Eq. (30), but the fourth length would be expected to be 8×10^{-8} cm rather than 3×10^{-7} cm.

This discrepancy appears to arise from the assumption implied in Eq. (28) that the dislocations are rigidly pinned at the pinning points. This is a good approximation for long loop lengths, but it is known[66] that the dislocations can also lean against the pinning points. In general, the compliance of the dislocations is make up of two parts, that arising from the displacement between the pinners and that arising from the displacement against the pinners as in a rigid rod. For short enough loop lengths, the former displacement becomes less important than the latter. Isaac and Granato[67] have given an expression for the frequency of a dislocation segment taking this into account which can be written as

$$\frac{1}{\omega^2}=\frac{L^2A}{\pi^2C}\left[\frac{L+L^*}{L}\right]\ , \tag{31}$$

where $L^*=\pi^2Cb^2/4U_0$ is of order of magnitude 10^{-6} cm for typical values of the constants with the pinning strength $U_0\sim0.1$ eV. The second term in Eq. (31), which becomes important only for small loop lengths, represents the contribution from the pinning-point compliance. When Eq. (31) is used in place of L^2A/π^2C in Eq. (28), one obtains a fit to the data with $L=8\times10^{-8}$ cm for $U_0=0.16$ eV. This is a reasonable value for the pinning-point energy. More data points would be needed to check Eq. (31) more thoroughly. This result also accounts for the observation[2] that the heaviest irradiation dose (180 000 R) does not restore the thermal conductivity to its predeformation value for $T\gtrsim3$ K. Furthermore, since the dislocations are nearly completely pinned ($L=8\times10^{-8}$ cm) at the heaviest dose, further irradiation would not be expected to decrease the dislocation scattering anymore.

Remaining minor discrepancies at low temperatures may be attributed to specular rather than diffuse scattering at the surface,[2] or to a small number of dipoles on the {101} planes. It was found, for example, that the freshly deformed sample data could be fit better by assuming a total density of 5×10^{8} cm^{-2} of which 0.5% were on the {101} planes. Discrepancies at temperatures greater than 2 K (and especially greater than 5 K) are attributed to processes neglected in our treatment—notably point-defect scattering and normal and umklapp processes. (See *Note added in proof.*) Roth and Anderson[2] indicated that heavy irradiation does not restore the thermal conductivity for $T>3$ K, although it is possible that the irradiation-induced point defects scatter significantly at these higher doses and temperatures.

In addition to fitting the experimental data, the model makes an interesting prediction of an effect which we will call the negative pinning effect. The normal effect of pinning is that after a heavy dose of irradiation the thermal conductivity of a deformed sample progressively recovers toward the undeformed sample value. The negative pinning effect is a *decrease* in thermal conductivity followed by the normal increase as the irradiation dose increases as illustrated in Fig. 13, where the normalized mean-free path is plotted versus normalized time βt [obtained from the relationship $L=L_0/(1+\beta t)$ with $L_0=2\times10^{-5}$ cm]. The negative pinning effect is a consequence of the underdamped character of the dislocation or dipole resonance so that the peak scattering rate due to short dislocations exceeds the high-frequency asymptote of longer dislocations as illustrated in Fig. 7. The negative pinning effect should be observed if the thermal conductivity of a deformed sample is continuously monitored during irradiation at constant temperature (e.g., 1 K).

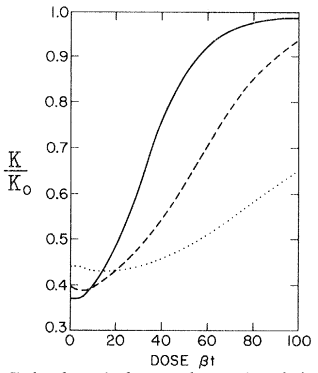

FIG. 13. Calculated thermal conductivity ratio κ/κ_0 at various temperatures vs time for constant irradiation rate. —: 0.6 K; — — —: 1 K; · · · : 2 K. The negative pinning effect is the decrease before recovery toward 1.

Finally we disagree with the statement of Matsuo and Suzuki[64] that scattering in LiF is not primarily due to vibrating dislocation dipoles below 3 K (based on Suzuki and Suzuki's[33] measurements in heavily deformed LiF). Suzuki and Suzuki did not measure at low enough temperatures to see the thermal conductivity minimum. Far above the minimum (i.e., the scattering-rate peak), the dislocations are inertia limited and scatter as if they were unpinned and uncoupled—regardless of dislocation length or spacing—so that one cannot discern between dipole and monopole scattering. As we have shown, the position of the minimum in Roth and Anderson's[2] data would require an anomalously short average dislocation length, unless they were mostly arranged in dipole configurations.

V. CONCLUSIONS

We have calculated the phonon scattering rates for dislocations and dislocation dipoles and have indicated the importance of specifically including the Ninomiya angle resonance effect, phonon focusing, and the resolved shear stress factor for each phonon. We have demonstrated that these factors do not conspire together to produce a large effect in [110] LiF, and that for a similar dislocation (or dipole) density the effect would be larger in [110] NaF. We have shown that the experimental data are fit with the assumption that a dislocation dipole density of 30 times the observed etch-pit density. We have predicted a negative pinning effect which is still to be confirmed experimentally. Finally we suggest that thermal conductivity studies in deformed alkali halides may be a good way to study very narrow dislocation dipoles.

Note added in proof. Recent unpublished work by R. A. Brown indicates that edge dipole strain-field scattering becomes increasingly important above 2 K in resolving the discrepancy between this present work and Roth and Anderson's[2] data.

ACKNOWLEDGMENT

Research supported by the National Science Foundation under Grant No. DMR80-15707.

---

*Present address: Xerox Webster Research Center, Webster, New York.

[1]A. C. Anderson and M. E. Malinowski, Phys. Rev. B 5, 3199 (1972).
[2]E. P. Roth and A. C. Anderson, Phys. Rev. B 20, 768 (1979).
[3]A. C. Anderson (unpublished).
[4]J. S. Koehler, in *Imperfections in Nearly Perfect Crystals,* edited by W. Shockley, J. H. Hollomon, R. Maurer, and F. Seitz (Wiley, New York, 1952), p. 197.
[5](a) A. Granato and K. Lücke, J. Appl. Phys. 27, 583 (1956). (b) A. Granato and K. Lücke, J. Appl. Phys. 27, 789 (1956).
[6]A. V. Granato and K. Lücke, in *Physical Acoustics,* edited by W. P. Mason (Academic, New York, 1966), Vol. 4A, p. 225.
[7]V. V. Nikolayev, Fiz. Metal. Metalloved. 18, 801 (1964).
[8]J. D. Eshelby, Proc. R. Soc. London A 197, 396 (1949).
[9]F. R. N. Nabarro, Proc. R. Soc. London A 209, 279 (1951).
[10]P. G. Klemens, Proc. Phys. Soc. London A 68, 1113 (1955).
[11]R. Berman, *Thermal Conduction in Solids* (Clarendon, Oxford, 1976).
[12]A. V. Granato, Phys. Rev. 111, 740 (1958).
[13]R. L. Sproull, M. Moss, and H. Weinstock, J. Appl. Phys. 30, 344 (1959).
[14]P. G. Klemens, in *Solid State Physics,* edited by F. Seitz and D. Turnbull (Academic, New York, 1958), Vol. 7, p. 1.
[15]P. Carruthers, Phys. Rev. 114, 995 (1959).
[16]P. Carruthers, Rev. Mod. Phys. 33, 92 (1961).
[17]J. M. Ziman, *Electrons and Phonons* (Clarendon, Oxford, 1960).
[18]H. Bross, Phys. Status. Solidi 2, 481 (1962).
[19]H. Bross, A. Seeger, and R. Haberkorn, Phys. Status. Solidi 3, 1126 (1963).
[20]H. Bross, A. Seeger, and P. Gruner, Ann. Phys. (N.Y.) 7, 230 (1963).
[21]A. Seeger, H. Bross, and P. Gruner, Discuss. Faraday Soc. 38, 69 (1964).
[22]P. Gruner, Z. Naturforsch. A 20, 1626 (1965).
[23]H. Bross, Z. Phys. 189, 33 (1966).
[24]M. Moss, J. Appl. Phys. 37, 4168 (1966).
[25]P. Gruner and H. Bross, Phys. Rev. 172, 583 (1968).
[26]K. Ohashi, J. Phys. Soc. Jpn. 24, 437 (1968).
[27]M. W. Ackerman and P. G. Klemens, Phys. Rev. B 3, 2375 (1971).
[28]Y. Kogure and Y. Hiki, J. Phys. Soc. Jpn. 38, 471 (1975).
[29]D. Eckhardt and W. Wasserbäch, Philos. Mag. A 37, 621 (1978).
[30]A. V. Granato, in *Internal Friction and Ultrasonic Attenuation in Crystalline Solids,* edited by D. Lenz and

K. Lücke (Springer, New York, 1975), Vol. 2, p. 33.
[31]S. Ishioka and H. Suzuki, Proceedings of the International Conference on Crystal Lattice Defects, Kyoto, 1962 [J. Phys. Soc. Jpn. 18, Suppl. II, 93 (1963).]
[32](a) T. Ninomiya, J. Phys. Soc. Jpn. 25, 830 (1968). (b) T. Ninomiya, in *Fundamental Aspects of Dislocation Theory,* edited by A. Simmons *et al.*, Natl. Bur. Stand. (U.S.) Spec. Publ. No. 317 (U.S. GPO, Washington, D.C., 1970), Vol. I, p. 315.
[33]T. Suzuki and H. Suzuki, J. Phys. Soc. Jpn. 32, 164 (1972).
[34]J. A. Garber and A. V. Granato, J. Phys. Chem. Solids 31, 1863 (1970).
[35]A. Taylor, H. R. Albers, and R. O. Pohl, J. Appl. Phys. 36, 2270 (1965).
[36]M. Moss, J. Appl. Phys. 36 3308 (1965).
[37]V. M. Zakharov, Fiz. Tverd. Tela Leningrad 9, 1514 (1967) [Sov. Phys.—Solid State 9, 1183 (1967)].
[38]H. Kaburaki, Y. Kogure, and Y. Hiki, J. Phys. Soc. Jpn. 49, 1106 (1980).
[39]G. Wire, Ph.D. thesis (University of Illinois, 1972) (unpublished).
[40]G. A. Kneezel, Ph.D. thesis (University of Illinois, 1980) (unpublished).
[41]H. B. G. Casimir, Physica 5, 495 (1938).
[42]M. Peach and J. S. Koehler, Phys. Rev. 80, 436 (1950).
[43]A. Granato and K. Lücke, J. Appl. Phys. 28, 635 (1957).
[44]J. D. Eshelby, Proc. R. Soc. London 266, 222 (1962).
[45]G. deWit and J. S. Koehler, Phys. Rev. 116, 1113 (1959); J. S. Koehler and G. deWit, Phys. Rev. 116, 1121 (1959).
[46]R. M. Stern and A. V. Granato, Acta. Metall. 10, 358 (1962).
[47]A. J. E. Foreman, Acta. Metall. 3, 322 (1955).
[48]H. B. Huntington, J. E. Dickey, and R. Thomson, Phys. Rev. 100, 1117 (1955).
[49]T. Laub and J. D. Eshelby, Philos. Mag. 14, 1285 (1966).
[50]R. E. Green and T. Hinton, Trans. Metall. Soc. AIME 236, 435 (1966).
[51]W. G. Johnston and J. J. Gilman, J. Appl. Phys. 30, 129 (1959).
[52]W. G. Johnston and J. J. Gilman, J. Appl. Phys. 31, 632 (1960).
[53]H. Strunk, J. Phys. (Paris) 38, 377 (1977).
[54]A. K. McCurdy, H.J. Maris, and C. Elbaum, Phys. Rev. B 2, 4077 (1970).
[55]H. J. Maris, J. Acoust. Soc. Am. 50, 812 (1971).
[56]B. Taylor, H. J. Maris, and C. Elbaum, Phys. Rev. B 3, 1462 (1971).
[57]G. A. Northrop and J. P. Wolfe, Phys. Rev. Lett. 43, 1424 (1979).
[58]A. H. Cottrell, *Dislocations and Plastic Flow in Crystals* (Oxford, London, 1953).
[59]T. R. Cass and J. Washburn, Proc. Br. Ceram. Soc. 6, 295 (1966).
[60]J. J. Gilman. See discussion following Ref. 31.
[61]R. W. Davidge and P. L. Pratt, Phys. Status. Solidi 6, 759 (1964).
[62]J. Washburn and T. Cass, J. Phys. (Paris) 27, Suppl. C3, 168 (1966).
[63]J. Hesse and L. W. Hobbs, Phys. Status. Solidi A 14, 599 (1972).
[64]T. Matsuo and H. Suzuki, J. Phys. Soc. Jpn. 43, 1974 (1977).
[65]A. V. Granato, A. Hikata, and K. Lücke, Acta. Metall. 6, 470 (1958).
[66]L. J. Teutonico, A. V. Granato, and K. Lücke, J. Appl. Phys. 35, 220 (1964).
[67]R. D. Isaac and A. V. Granato (unpublished).